High-resolution local vibrational mode spectroscopy and electron paramagnetic resonance study of the oxygen-vacancy complex in irradiated germanium

P. Vanmeerbeek, P. Clauws, and H. Vrielinck
Department of Solid State Sciences, Ghent University, Krijgslaan 281-S1, B-9000 Gent, Belgium

B. Pajot
GPS, UMR 7588, Université Pierre et Marie Curie, Campus Boucicaut, 140 rue de Lourmel, 75015 Paris, France

L. Van Hoorebeke
Department of Subatomic and Radiation Physics, Ghent University, Proeftuinstraat 86, B-9000 Gent, Belgium

A. Nylandsted Larsen
Institute of Physics and Astronomy, University of Aarhus, Ny Munkegade, DK-8000 Aarhus C, Denmark
(Received 26 March 2004; revised manuscript received 30 April 2004; published 13 July 2004)

It was recently discovered that in electron-irradiated germanium doped with oxygen a local vibrational mode occurs at 669 cm^{-1} that could be ascribed to the negatively charged oxygen-vacancy complex (VO^-). In the 669 cm^{-1} band and in another unassigned band at 731 cm^{-1} due to a different defect, fine structures indicating the occurrence of a germanium isotope splitting of the modes could be partly resolved. We report here the results of high-resolution (=0.02 cm^{-1}) infrared measurements at liquid helium temperature of bands at 635, 669, 716, and 731 cm^{-1}. In this work, the experimentally observed splitting of all four local vibrational modes and the amplitudes of the individual components within each mode are accurately predicted from a nonlinear symmetric Ge−O−Ge quasimolecule embedded in the germanium lattice. Electron paramagnetic resonance measurements have also been performed on an O doped ^{74}Ge quasi monoisotopic sample after electron irradiation. The symmetry of the dominant paramagnetic defect in the sample is found to be orthorhombic I and the principal *g* values are in good agreement with those reported earlier for the VO^- center. Through annealing (at 120 °C) a correlation can be made between the intensity of this electron paramagnetic resonance signal and the infrared band at 669 cm^{-1}, giving explicit support to earlier identifications of these signals as due to VO^-.

DOI: 10.1103/PhysRevB.70.035203 PACS number(s): 61.80.Fe, 63.20.Pw, 61.72.Tt

I. INTRODUCTION

The oxygen-vacancy (VO) defect is one of the dominant defects produced by room temperature (RT) irradiation of O doped Ge. The defect forms through trapping of mobile vacancies (induced by irradiation) by interstitial O atoms (O_i). It is generally accepted that in Si (Ref. 1) and Ge, the VO defect has orthorhombic symmetry, with the O atom bonded to two of the four Si or Ge nearest neighbor atoms surrounding the vacancy, while a reconstructed bond is formed between the remaining unpaired atoms. In Ge, this conclusion was drawn in 1964 from electron paramagnetic resonance (EPR) measurements[2] on electron-irradiated O doped samples. This reference included also a comparison of the intensity changes of electron-induced infrared local vibrational modes (LVM's) and of the VO EPR signal under thermal annealing. However a clear correlation between some of the LVM's and the VO center in Ge was only published in 1965, when Whan suggested from her thorough IR investigation that a LVM at 620 cm^{-1} was associated with the VO center.[3] In a recent EPR study[4] on quasimonoisotopic (QMI) ^{74}Ge a slightly different g value in the ⟨100⟩ direction was reported for the VO^- defect as compared to that of the former EPR study.

Only recently it was reported[5] that the VO center in Ge doped with ^{16}O is responsible for at least two LVM's at 620 and 669 cm^{-1}, assigned to VO^0 and VO^- respectively, while another study[6] argues that a third LVM at 716 cm^{-1} is related to VO^{2-}. This implies that, as in Si, the frequency of the stretching mode of the VO center in Ge depends on the charge state of the defect. *Ab initio* calculations[7] of the bond lengths and angle of VO in Ge predict a very small shift of these quantities and of the stretch frequency between VO^0 and VO^-. We reported in a previous study[5] that the LVM at 669 cm^{-1} assigned to VO^- and a yet unassigned band at 731 cm^{-1} exhibit fine structure near liquid helium temperatures (LHeT), probably as a consequence of Ge isotope splitting. However, a detailed study of the fine structure could not be made with the resolution available. In this paper we report on the investigations with high-resolution of the LVM's at 635, 669, 716, and 731 cm^{-1}, followed by a study of the observed fine structure and a new combined EPR, IR study of the VO^- defect using monoisotopic ^{74}Ge.

II. EXPERIMENTAL DETAILS

Five O doped Ge samples were used in this study. Prior to irradiation, they were subjected to a 5 min oxygen dispersion treatment at 900 °C followed by a quench to RT, in order to anneal out any uncontrolled defect formed during the cooling-down of the crystal. The O_i concentration was mea-

TABLE I. Characteristics of the Ge:O samples investigated including the 2 MeV electron fluences. Samples A, B, C, and D come from natural material and sample E from qmi ^{74}Ge material. The O_i concentration in sample A is for ^{18}O.

Sample	$[O_i]$ (cm^{-3})	Fluence (cm^{-2})	Post-irradiation treatment
A	3.3×10^{16}	3.8×10^{17}	None
B	2.5×10^{17}	3.8×10^{17}	None
C	2.9×10^{17}	1.5×10^{16}	None
D	2.7×10^{17}	5.0×10^{17}	120–240 °C anneals
E	3.3×10^{15}	3.8×10^{17}	None

sured after the quench and determined from the peak absorption of the ν_3 mode at RT, using a conversion factor[8] of 5×10^{16} cm^{-2}. Sample A was doped with ^{18}O to an O_i concentration of 3.3×10^{16} cm^{-3}, the $^{16}O_i$ concentration being about six times lower. Samples A, B, C, and D were ideally prepared for IR measurements in order to detect LVM's at 635, 669, 716, and 731 cm^{-1}, respectively. Sample E was prepared primarily for EPR measurements. All samples were irradiated with 2 MeV electrons and the temperature of the samples during irradiation was kept close to RT in order not to anneal out the VO centers produced. Sample C received a second heat treatment at 350 °C for several hours in flowing argon before irradiation. This treatment was intended to produce thermal donors in order to increase the free electron concentration for trapping by VO to produce VO^{2-} during irradiation. The irradiation dose for this sample was kept low in order to keep the electrons trapped on VO^{2-}. Isochronal anneals of 20 min. at 120, 160, 200, and 240 °C were performed on sample D in flowing argon to get a high absorption of the 731 cm^{-1} band, in accordance with our previous study[5] The different experimental details of all samples are shown in Table I.

The IR spectra were recorded with a Bruker IFS66v FT spectrometer for the determination of the O_i concentration at RT (resolution = 1.0 cm^{-1}) and with a BOMEM DA3+ FT spectrometer for the high-resolution measurements at LHeT.

X-band (ν=9.57 GHz) EPR measurements on sample E were performed at 40 K using a Bruker ESP300E spectrometer equipped with an Oxford ESR10 cryostat, before and after a thermal treatment of 20 min. at 120 °C. DPPH (2,2-diphenyl-1-picrylhydrazyl) was measured for field calibration. The long axis of sample E is oriented along a ⟨110⟩ direction, which allowed the angular dependence of the spectra to be recorded in a (110) plane.

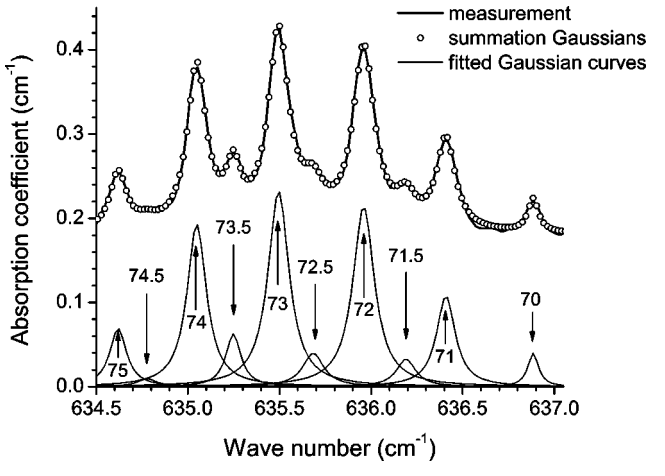

FIG. 1. Absorption of the LVM at 635 cm^{-1} in sample A at LHeT. The resolution is 0.04 cm^{-1}. This LVM is the ^{18}O counterpart of the ^{16}O LVM at 669 cm^{-1} shown in Fig. 2. The arrows indicate the average or true masses of the two Ge neighbors of the O atom.

III. EXPERIMENTAL RESULTS AND DISCUSSION

A. FTIR spectra

High-resolution spectra of the bands at 635, 669, 716, and 731 cm^{-1} at LHeT are shown in Figs. 1, 2, and 5, and 7. The solid curves in the upper half of the figures correspond to the experimental spectra and they are shifted upwards for clarity. The lower part of the figures shows the Gaussian curves fitted to the spectrum. The open circles represent summation of the Gaussian curves and are also shifted upwards for clarity. The fine structure of the bands bears some resemblance to the high-resolution spectra of the ν_3 antisymmetric stretch mode of interstitial oxygen.[9]

The splitting of the O_i band arises from the rotation of the O atom around the Ge—Ge axis of the quasimolecule on the one hand and from the different isotopic ^{n}Ge-^{m}Ge combina-

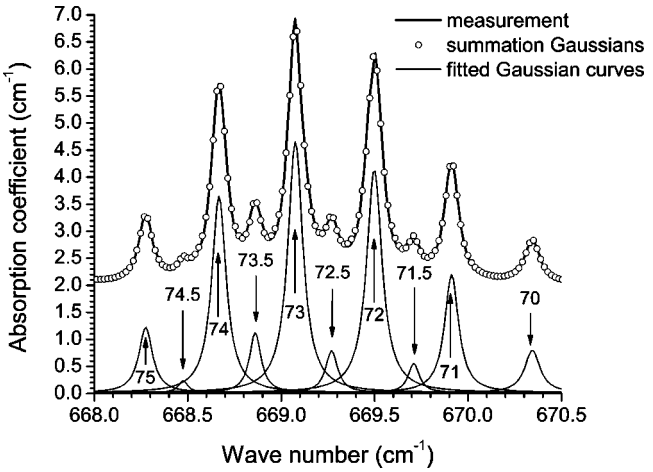

FIG. 2. Absorption of the LVM at 669 cm^{-1} in sample B at LHeT. The resolution is 0.02 cm^{-1}. The arrows have the same meaning as in Fig. 1.

TABLE II. Relative intensities of bands corresponding to different ^{n}Ge-^{m}Ge combinations based on the abundances of natural Ge.

$\langle M_{av} \rangle$	Combination *n-m*	Predicted intensity (%)
70	70−70	4.2
71	70−72	11.3
71.5	70−73	3.2
72	70−74, 72−72	22.5
72.5	72−73	4.3
73	70−76, 72−74, 73−73	23.8
73.5	73−74	5.7
74	72−76, 74−74	17.6
74.5	73−76	1.2
75	74−76	5.7
76	76−76	0.6

tions on the other hand. In the case of QMI ^{74}Ge, the rotation of the O atom resulted in four observable vibration-rotation lines near LHeT.[10,11] A similar rotational splitting is expected for every distinct ^{n}Ge-^{m}Ge combination. Thus in natural Ge, where 15 different Ge_2O combinations occur (the isotopic abundances (%) of natural Ge are ^{70}Ge: 20.52, ^{72}Ge: 27.43, ^{73}Ge: 7.76, ^{74}Ge: 36.54, ^{76}Ge: 7.76), 60 vibration-rotation lines are predicted in the spectrum of the $\nu_3(^{16}O)$ mode. However, some of the ^{n}Ge-^{m}Ge combinations have the same average mass (e.g., $^{73}Ge_2$-O and ^{70}Ge-O-^{76}Ge) as a result of which the corresponding transitions will be difficult to distinguish. It is also possible that some of the four vibration-rotation lines of a given ^{n}Ge-^{m}Ge combination coincide with a vibration-rotation line of another ^{n}Ge-^{m}Ge combination. For these reasons only 25 individual lines in the ν_3 antisymmetric stretch mode of O_i could be resolved in the most recent experiments.[12]

1. The 635 *and* 669 cm^{-1} *bands*

The LVM's at 635 and 669 cm^{-1} have previously been assigned[5,13,14] to the VO^- defect in Ge crystals doped with ^{18}O and ^{16}O, respectively. At a difference with the ν_3 vibrational structure of O_i, the absence of fine structure for each isotopic combination of VO^- seems to indicate that no rotation of the O atom takes place in this defect. This means that the fine structure we observe can probably be ascribed only to the different ^{n}Ge-^{m}Ge combinations. To check this assumption we have plotted the predicted relative intensities of the individual components given in Table II and based on the isotopic abundances of natural Ge against the integrated absorption of the fitted Gaussian curves for the two bands. The results are shown in Figs. 3 and 4. The graphs indicate that there is a clear linear dependence between the two quantities for the two bands. The fact that the fitted lines do not exactly pass through the origin of the graphs can be ascribed to the used baseline corrections in the spectra. The linear dependence is a first indication that the defects responsible for absorption at 635 and 669 cm^{-1} are both due to an O atom bonded to two equivalent Ge atoms and this is consistent with the earlier assignments.

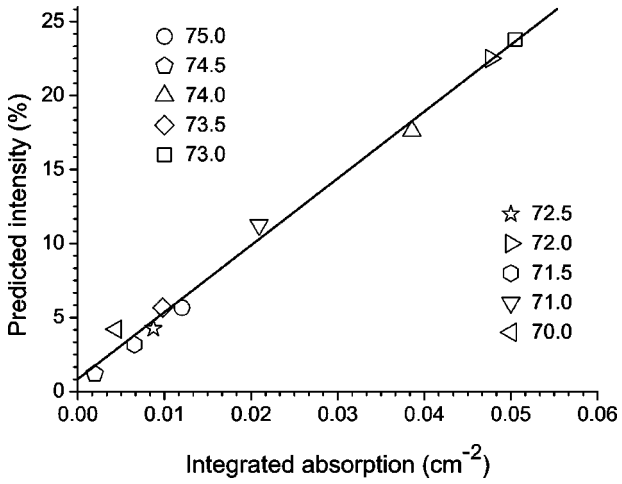

FIG. 3. Integrated absorption vs predicted intensity of the band at 635 cm^{-1}. The different modes are indicated by their average Ge masses.

To further check whether the fine structure of the bands can be ascribed to a nonlinear symmetric Ge—O—Ge molecule in a Ge crystal lattice we calculated the isotopic shifts[15] of the ν_3 mode of such a quasimolecule from Eq. (1) by a best-fit procedure:

$$\frac{\nu_3(^{k}Ge_2{}^{l}O)}{\nu_3(Ge_2O)} = \sqrt{\frac{M_{Ge}M_O(M_{l_O} + 2M_{k_{Ge}}\sin^2\alpha)}{M_{k_{Ge}}M_{l_O}(M_O + 2M_{Ge}\sin^2\alpha)}}. \quad (1)$$

In this equation, M_X stands for the mass of atom X, ^{k}Ge or ^{l}O stands for an isotope of Ge or O and 2α stands for the apex angle of the nonlinear symmetric Ge—O—Ge molecule. In the case of inequivalent isotopic substitutions of the two Ge atoms, it has been shown[9] that the asymmetric quasimolecule ^{M_1}Ge—O—^{M_2}Ge is equivalent to ^{M_3}Ge—O—^{M_3}Ge, where M_3 is the arithmetic mean of M_1 and M_2. If no prefix is used in Eq. (1), we mean the Ge or O atom used as reference relative to which all the wave num-

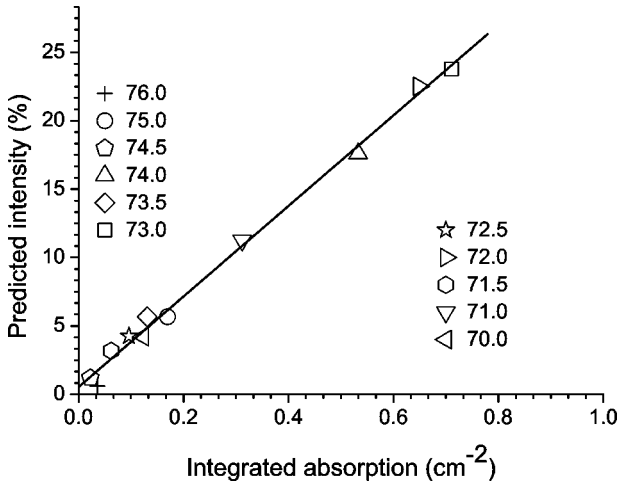

FIG. 4. Integrated absorption vs predicted intensity of the band at 669 cm^{-1}. The different modes are indicated by their average Ge masses.

TABLE III. Comparison of the experimental *Ge* isotope shifts of the 635 and 669 cm^{-1} bands with those calculated from from Eq. (1) with $2\alpha=102°$, $m'=23$ amu. The reference is $\langle M_{av}\rangle=71$ amu.

	635 cm^{-1} band		669 cm^{-1} band	
$\langle M_{av}\rangle$	Exp.	Calc.	Exp.	Calc.
70	636.88	636.87	670.34	670.35
71	636.41	636.41	669.91	669.91
71.5	636.19	636.18	669.71	669.69
72	635.96	635.95	669.50	669.48
72.5	635.68	635.73	669.27	669.26
73	635.50	635.50	669.08	669.05
73.5	635.25	635.28	668.86	668.84
74	635.05	635.06	668.67	668.64
74.5	634.78	634.85	668.48	668.43
75	634.62	634.63	668.28	668.23
76	-	-	667.88	667.83

bers are calculated. In the case of Ge isotopic shifts, we choose for this reference the ^{70}Ge—^{16}O—^{72}Ge quasimolecule, labeled as $\langle M_{av}\rangle=71$ in Tables III and V.

Because the quasimolecule is embedded in the crystal we also take into account an interaction mass m' empirically added to the Ge atom mass. Thus in Eq. (1), M_{Ge} (with or without prefix) should be replaced with $M_{Ge}+m'$. With the equation, we can calculate the shift in wave numbers due to the substitution of a Ge or an O atom in the Ge—O—Ge quasimolecule. For the two bands involved, the couple: interaction mass and apex angle $(m';2\alpha)$ is determined through a best-fit procedure of the theoretical calculated LVM's to three experimental datasets. These three datasets are (1) the wave number shifts due to a Ge substitution in the 635 band assigned to $V^{18}O^-$, (2) the wave number shifts due to a Ge substitution in the 669 band assigned to $V^{16}O^-$, (3) the wave number shifts between components of the 635 and the 669 bands due to O substitution. As a result of the fitting procedure to the three datasets, we can calculate all wave number shifts with the couple ($m'=23$ amu ; $2\alpha=102°$) for the two bands, as can be seen from Table III. The error of such a fitting procedure on the 2α value is estimated at around 2%. This estimate was found through comparison of the fitted 2α values obtained by applying the best-fit procedure to each of the above datasets separately.

TABLE IV. Comparison of the geometrical parameters of VO^- in Ge as deduced from the Ge isotope effect of the 635 and 669 cm^{-1} LVM's and from the *ab initio* calculations of Ref. 7. *V* denotes the center of the vacancy. Labels of Ge atoms are those of Fig. 11. The second nearest neighbor distance in Ge is 4.00 Å.

	This work	Ref. 7
Ge_c—O—Ge_b apex angle (degrees)	102	152
Ge—O bond length (Å)	1.74	1.79
Ge_c—Ge_b distance (Å)	2.70	3.46
O—V distance (Å)	0.33	1.14

TABLE V. Isotopic shifts for the 716 and 731 cm^{-1} bands; experimental wave numbers vs calculated wave numbers. Upper part of the table: Ge isotopic shifts. Lower part of the table: O isotopic shifts.

	716 cm^{-1} band		731 cm^{-1} band	
$\langle M_{av}\rangle$	Exp.	Calc.[a]	Exp.	Calc.[b]
70	717.58	717.56	732.94	732.95
71	717.12	717.12	732.50	732.50
71.5	716.96	716.90	732.28	732.27
72	716.72	716.68	732.06	732.05
72.5	716.52	716.46	731.85	731.83
73	716.26	716.25	731.62	731.61
73.5	716.06	716.04	731.40	731.40
74	715.80	715.83	731.19	731.19
74.5	715.58	715.62	730.96	730.98
75	715.41	715.41	730.78	730.77
Natural Ge	Exp.	Calc.	Exp.	Calc.
^{16}O	716.2[c]	716.20	731.4[c]	731.40
^{18}O	680.4[c]	679.98	694.0[d]	694.00

[a]Calculated from Eq. (1) with $2\alpha=107°$, $m'=23$ amu.
[b]Calculated from Eq. (1) with $2\alpha=123°$, $m'=16$ amu.
[c]Reference 13.
[d]Reference 19.

The fitting procedure with Eq. (1) indicates that the 635 and the 669 cm^{-1} bands belong to the same nonlinear Ge—O—Ge defect and that the observed fine structure can be ascribed only to the vibration of the involved molecules and not to rotation. Both observations are in agreement with the model of the VO defect, where the O atom is bonded to two equivalent Ge atoms without the possibility for the O atom to rotate around the Ge—Ge axis.

With the fitted apex angle and the assumption[9] that the distance between the Ge and the O atom remains the same as in GeO_2 (1.74 *Å*) we may calculate the different bond lengths in the VO^- defect. The results are shown in Table IV. We find that the O atom is moved away from the vacancy site by an amount of only 0.33 *Å*, while the two nearest neighbor Ge atoms are drawn closer to each other (compared to a perfect Ge crystal and assuming that the Ge—Ge axis is unchanged). The O atom is thus placed near the substitutional site and this picture is different from that of the theoretical study[7] where the distance between the O atom and the vacancy was found to be 1.14 *Å* (placing the O atom near the axis of the nearest Ge neighbors). The apex angle for the VO^- defect in the theoretical study was also found to be larger.

2. The 716 cm^{-1} band

As mentioned in Sec. II, special care was taken in order to produce the 716 cm^{-1} band. Since the band has been ascribed[6] to the VO^{2-} defect, it can only be observed in an *n*-type irradiated O doped Ge sample. We therefore induced

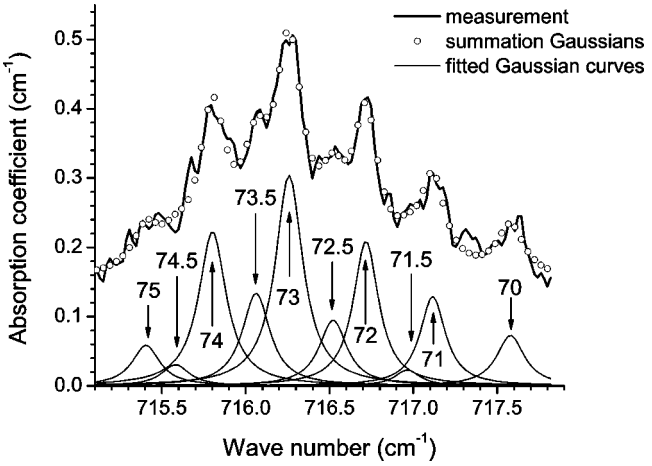

FIG. 5. Absorption of the LVM at 716 cm^{-1} in sample C at LHeT. The resolution is 0.16 cm^{-1}. The arrows have the same meaning as in Fig. 1.

thermal donors into a quenched sample by thermal treatment. This sample received a much lower electron irradiation dose than the others, because according to Refs. 16–18, the Fermi level is pinned to the $E_v+0.27$ eV level in highly irradiated O doped Ge. Thus a high irradiation dose would result in an *n*- to *p*-type conversion. The high-resolution IR measurement of the peak can be seen in Fig. 5. The quality of the spectrum is not as good as for the other spectra presented in this article. The reason for this is the combination of a rather low concentration of VO^{2-} as a consequence of the low irradiation dose, and the presence of free carrier absorption in this particular wave number range due to the presence of thermal donors. Nevertheless, one can see in Fig. 5 that the band also displays a fine structure which resembles the Ge isotope splitting. In Fig. 6 we again plotted the integrated absorption of the fitted Gaussian curves versus the expected intensity and it is fitted with a linear relationship. The larger scattering of the data points as compared to Figs. 3 and 4, and 8 results from the larger noise of the spectrum of sample C.

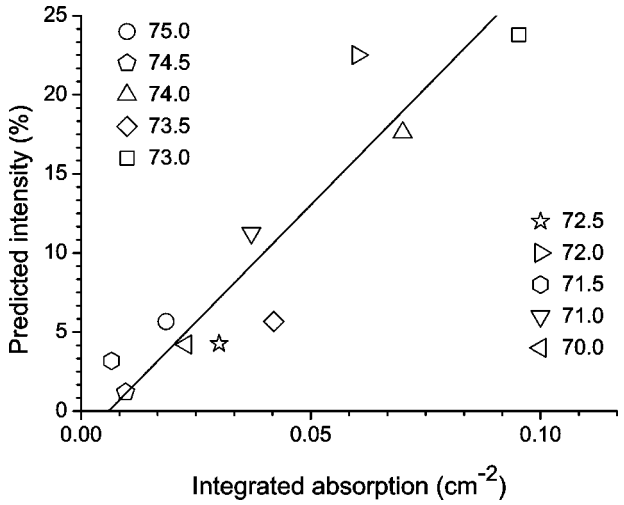

FIG. 6. Integrated absorption vs predicted intensity of the band at 716 cm^{-1}. The different modes are indicated by their average Ge masses.

If we are indeed dealing with a Ge-Ge isotopic fine structure in the band, then we should be able to calculate the different isotopic shifts from Eq. (1), again through a best-fit procedure. No spectrum of the ^{18}O counterpart of the 716 cm^{-1} mode (and also of the 731 cm^{-1} band discussed below) has been obtained in the present study. In such a situation, it is impossible to find a unique $(m'\ ;\ 2\alpha)$ set from the ^{16}O mode alone. A low-resolution ^{18}O counterpart of the 716 cm^{-1} band has been reported[13] at 680.4 cm^{-1}. However, this latter value is derived from an absorption band without a clear peak position and should therefore not be used in a high-accuracy fitting procedure. In order to get a unique set $(m'\ ;\ 2\alpha)$ we use the value of m' obtained above for the VO^- defect. The reason for this is that since m' represents the binding of the quasimolecule to the crystal, this parameter should not vary much with the charge state of the defect. Keeping $m'=23$ amu results then in $2\alpha=107°$. The agreement between calculated and experimental positions of the Ge isotopic lines using these values of the parameters is obvious from Table V. Furthermore, with the same values and using the low-resolution position of 716.2 cm^{-1} for the $V^{16}O^{2-}$ LVM given in Ref. 13, the position of the $V^{18}O^{2-}$ band is predicted at 679.98 cm^{-1}, close to the observed value 680.4 cm^{-1}.

Comparing the 2α values of the VO^- and the VO^{2-} defect, we see that they differ by about 5%. This relative difference only exceeds the predicted accuracy of the difference between two 2α values $(2\times 2\%=4\%)$ by a small amount and thus care should be taken on the conclusions drawn. If the slightly larger value for 2α in VO^{2-} is significant, we can conclude that the extra electron places the O atom somewhat further away from the substitutional site, indicating that the O atom moves closer to the Ge—Ge axis as the defect gets more negatively charged. Apparently the extra electron in the reconstructed Ge—Ge bond pushes to O atom further away from the center of the vacancy.

In this respect it should be mentioned that the present high-resolution experiments confirm our earlier observation that the LVM band at 620 cm^{-1} ascribed to the VO^0 defect displays no fine structure as found for the VO^- and VO^{2-} bands. Furthermore, no fine structure is seen in the equivalent $V^{18}O^0$ counterpart at 590 cm^{-1}. We may only speculate on the origin of this lack of fine structure. Perhaps the lack of an extra electron in VO^0 places the O atom even closer to the substitutional site, consistent with the idea that extra electrons in the Ge—Ge bond of VO push the O atom further away from the vacancy site. In the case of VO^0 we may then be concerned with a more Ge_4O-like molecule instead of a Ge_2O-like molecule. The high number of Ge isotopic combinations may then lead to unresolvable bands.

3. The 731 cm^{-1} *band*

We know from our earlier study[5] that the defect responsible for the 731 cm^{-1} band cannot be associated with the VO defect because it has a very different annealing behavior. This is the reason why, in order to form the defect, we submitted the sample to a thermal treatment as described in Sec. II. The result of the Gaussian curve fitting to the high-

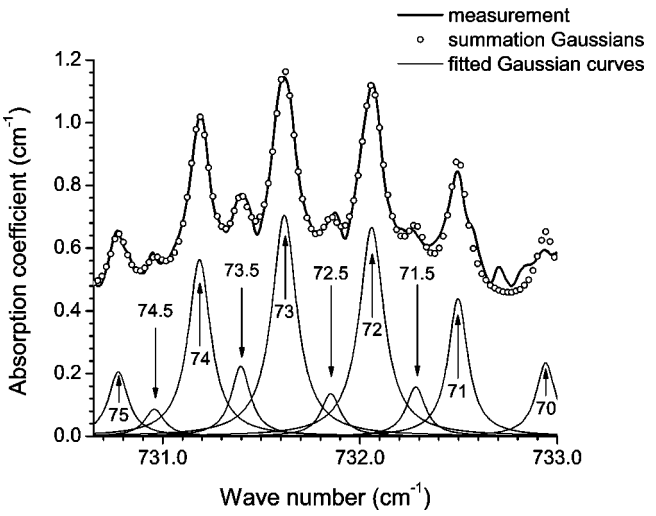

FIG. 7. Absorption of the LVM at 731 cm^{-1} in sample D at LHeT. The resolution is 0.05 cm^{-1}. The arrows have the same meaning as in Fig. 1.

resolution measurement and the plot of integrated absorptions of the fitted Gaussian curves versus the expected intensities if we are again assuming a Ge isotope splitting can be seen in Figs. 7 and 8. Again, the linear dependence in Fig. 8 is striking. A best-fit procedure (similar to the ones described above) to the experimental LVM's of the band yields $m'=16$ amu and $2\alpha=123°$. Table V shows that the difference between the experimental and the calculated LVM's of this band with this couple is small. As in the case of the 716 cm^{-1} band we needed extra information to obtain the unique couple $(m';2\alpha)$, this extra information was given by the fact that the ^{18}O counterpart of the 731 cm^{-1} band is known to have[19] a LVM at 694.0 cm^{-1}. We may conclude that the spectrum of the 731 cm^{-1} band clearly exhibits Ge isotope splitting and this is an indication that the defect responsible for the 731 cm^{-1} band must resemble a Ge—O—Ge quasimolecule. Regarding the higher formation temperature of the band, the most straightforward identification might thus be

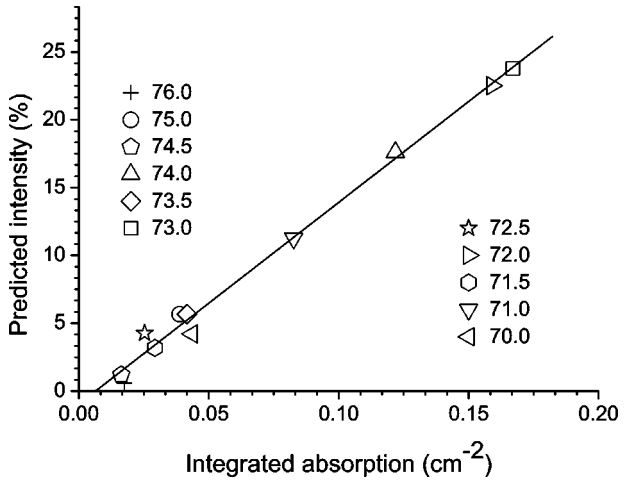

FIG. 8. Integrated absorption vs predicted intensity of the band at 731 cm^{-1}. The different modes are indicated by their average Ge masses.

TABLE VI. Comparison of the principal g values corresponding to the VO^- defect.

g values	Baldwin[a]	Khirunenko[b]	This study
$g_{x,\|\|\langle 0\bar{1}1\rangle}$	2.0046±0.0010	2.0044	2.0046±0.0008
$g_{y,\|\|\langle 100\rangle}$	2.0098±0.0010	2.0081	2.0081±0.0006
$g_{z,\|\|\langle 011\rangle}$	2.0426±0.0010	2.0431	2.0428±0.0006

[a]Reference 2.
[b]Reference 4.

that the band is related to a $V_nO(n>1)$ center. However, we should keep in mind that in Si, the VO_2 defect can be considered as two practically independent Si—O—Si defects with main axes mutually orthogonal sharing the same vacancy.[20] Hence, an attribution of the 731 cm^{-1} band to VO_2 does not contradict the Ge—O—Ge quasimolecule assumption.

B. EPR study of VO^-

1. Earlier studies

EPR measurements of the VO^- defect in Ge have been performed before.[2,4] However, there exists a small discrepancy between the articles concerning the g value of the defect in the $\langle 100\rangle$ direction. The study by Baldwin[2] was performed on natural Ge. It was concluded that a paramagnetic center with $S=1/2$, present after irradiation, was due to the VO^- defect. The assignment was based on the observation that in Si the dominant defect after irradiation is the VO center and the similarity of the observed g shifts of the center in Ge with those of the VO center in Si, taking into account the different spin-orbit coupling constants. The study also included an annealing experiment in which the evolution of seven LVM's was monitored. One of the conclusions was that the defect responsible for the EPR signal is not associated with the 715 cm^{-1} band.

The results presented in Ref. 4 were obtained on QMI ^{74}Ge and the changes in the EPR signals corresponding to VO^- and divacancies (V_2) were examined as a function of annealing. It is, however, not clear which of the g values listed in this reference belong to the V_2 and the VO^- centers. Through similarity with the data presented by Baldwin, we believe we have selected the g values belonging to the VO^- center. Within experimental error the g values for both experiments, shown in Table VI, are in agreement except for the $g_{y,\|\langle 100\rangle}$ value.

2. EPR spectrum of VO^-

As mentioned in Sec. II we used QMI ^{74}Ge for the present EPR study. The ^{73}Ge concentration in this QMI sample is thus very small and the broadening of the EPR lines due to the spin 9/2 and the large nuclear momentum of this isotope is virtually absent,[4] allowing an accurate analysis of the EPR signals.

The results of our EPR measurements can be seen in Fig. 9, where the EPR spectra in both the $\langle 110\rangle$ and the $\langle 100\rangle$

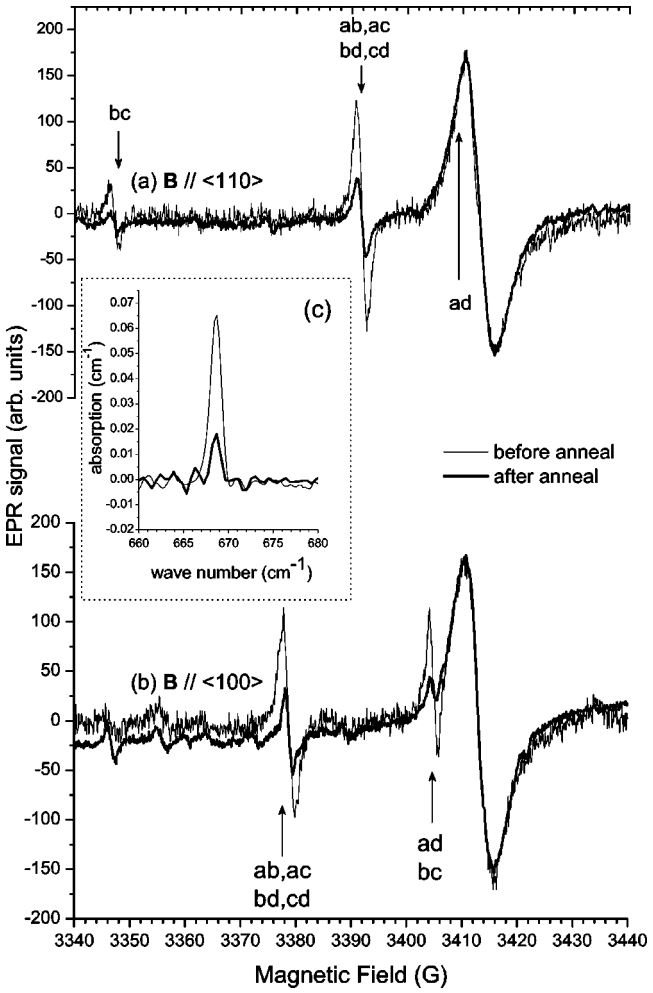

FIG. 9. Actual EPR signal of VO^- before and after annealing at 120 °C for 20 min. with magnetic field in (a) the ⟨110⟩ and (b) the ⟨100⟩ directions. The inset (c) shows the evolution of the IR absorption of the band at 669 cm^{-1} before and after the anneal.

directions are plotted before and after the anneal. The number of scans in the spectrum after the anneal is ten times higher in order to get a reasonable signal to noise ratio for the VO^- signal. As a result, the general noise level of the second spectrum is lower by a factor of 3. The EPR signals of the paramagnetic center, corresponding to the different orientations of VO^- defined in Fig. 11, are indicated by arrows. The large EPR signal centered around 3412 G, which does not evolve during the annealing, is related to the EPR cavity and may be used as a reference for the signal height.

Although sample E was primarily prepared for EPR measurements, we could measure IR absorption at 669 cm^{-1}. The inset of Fig. 9 shows the absorption spectrum of the band before and after the anneal. A high-resolution IR measurement of this LVM was not performed due to the rather low absorption coefficient. Based on the position, the line shape and the annealing behavior, we have no doubt that this LVM is exactly the same as the one described in Sec. III A 1. A comparison between the evolution of the 669 cm^{-1} band and the evolution of the EPR signal, as a consequence of the thermal treatment, shows that in both cases the signals decrease by a factor of 3 to 4. The EPR signal from Ref. 2

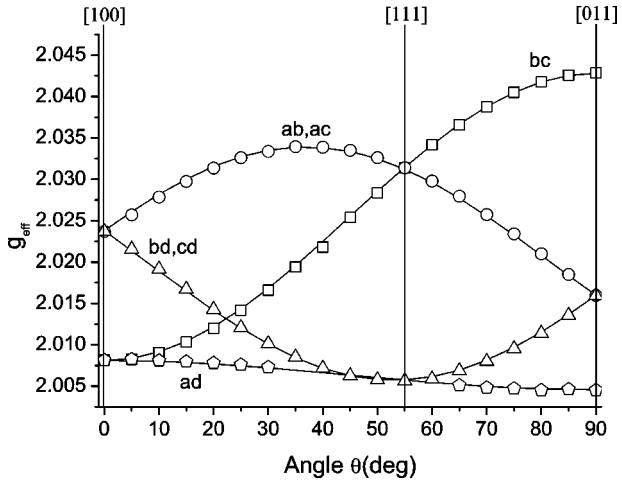

FIG. 10. Angular dependence of the principal g values of the VO^- EPR spectrum for the magnetic field **B** rotating in the $(0\bar{1}1)$ plane. The labels correspond to the six different orientations of the defect in accordance with Fig. 11. The markers represent the actual experimental data, the solid lines are fitted to the data.

showed exactly the same annealing behavior after a heat treatment of 125 °C for 40 min.

The similar annealing behavior of the EPR signal ascribed to the VO^- defect[2] and the LVM at 669 cm^{-1} is a confirmation of the earlier assignment of the 669 cm^{-1} band to VO^-. In this respect, the conclusion drawn by Baldwin[2] that the EPR signal is not associated with the 716 cm^{-1} band is correct.

Figure 10 shows the angular variation of the EPR signal for rotation of the magnetic field in the $(0\bar{1}1)$ plane. The angular dependence of the principal g values is typical for a defect which exhibits orthorhombic I symmetry. The six different defect orientations are labeled in accordance with Fig. 11. Because we are measuring in a (110)-symmetry plane of the defect, the resonances of the orientations ab, ac and bd, cd coincide. This symmetry is reflected in the g tensor.

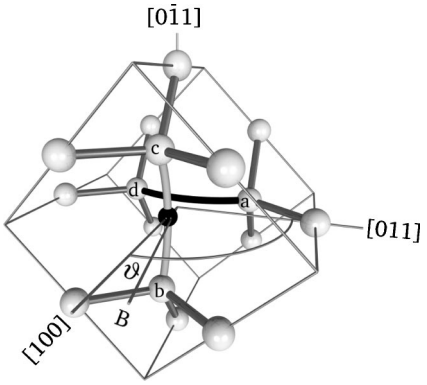

FIG. 11. Model of the negatively charged oxygen-vacancy defect in Ge. A white sphere represents a Ge atom while the black sphere represents the O atom. The latter is slightly displaced from the substitutional site along a ⟨100⟩ direction. The defect is shown in the standard orientation ad. In this orientation, the defect electron is mainly localized in the reconstructed dangling bond between the atoms a and d.

The principal values of the latter were calculated by a computer fit of the measured magnetic resonance fields to the equation $H=\mu_B\vec{B}\cdot\overleftrightarrow{g}\cdot\vec{S}$, which accounts for the interaction between the unpaired electron of the defect and the magnetic field. The principal values obtained in this study are given in the last column of Table VI. We can conclude that the $g_{x,\|\langle 0\bar{1}1\rangle}$ and $g_{z,\|\langle 011\rangle}$ values following the three studies are in excellent agreement with each other. As for the $g_{y,\|\langle 100\rangle}$ value, this study confirms the value presented by Khirunenko.[4] The difference in $g_{y,\|\langle 100\rangle}$ value from Baldwin[2] can probably be related to the fact that the value was derived from a study using natural Ge, resulting in an EPR spectrum with broader linewidths.

IV. CONCLUSION

Reinvestigation of the IR absorption bands at 669 and 731 cm^{-1} with high-resolution measurement confirms the proposed model[5] that both defects contain a single O atom bonded to two equivalent Ge neighbors. We emphasize that the two LVM bands belong to different defects. The 669 cm^{-1} band is ascribed to the VO^- defect while the 731 cm^{-1} band is ascribed to either a V_nO $(n>1)$ or a VO_2 defect. The fine structure observed in the 669 cm^{-1} band is also found in the ^{18}O counterpart located at 635 cm^{-1}. It is consistent with the assignment of the latter two bands to the same VO^- defect.[5,13]

We find that the observed fine structure in the high-resolution measurement of the 716 cm^{-1} band can also be ascribed to a defect with a single O atom bonded to two equivalent Ge neighbors. This confirms the earlier assignment[6] of the band to the VO^{2-} defect.

All these conclusions are based on the comparison of the predicted relative intensities of the different components with the integrated absorption of the individual components observed, together with verification that the Ge or O isotope shifts of these modes can be predicted accurately with a two-parameter $(m';2\alpha)$ semiempirical model. With the fitted apex angle (2α) we can make an estimate of the bond lengths and angles within the defects. In the case of the VO^- and the VO^{2-} center we find that the average position of the O atom would be closer to the substitutional site than it was concluded before.[7]

An EPR study of a paramagnetic center in irradiated O doped QMI ^{74}Ge, together with an IR study using the same sample resulted in strong proof to correlate the EPR signal of the VO^- defect with the LVM at 669 cm^{-1}. From the angular variation of the EPR spectra, the paramagnetic center was shown to have orthorhombic I symmetry with principal g values in close agreement with those of earlier studies.[2,4]

ACKNOWLEDGMENTS

We are greatly indebted to Professor J. L. Lindström for providing the ^{18}O enriched material and to L. Khirunenko for the QMI $^{74}Ge:O$ material.

[1] G. D. Watkins and J. W. Corbett, Phys. Rev. **121**, 1001 (1961).
[2] J. A. Baldwin, Jr., J. Appl. Phys. **36**, 793 (1965).
[3] R. E. Whan, Phys. Rev. **140**, A690 (1965).
[4] L. Khirunenko, N. Tripachko, V. Shakhovtsov, V. Yashnik, and V. Shumov, Mater. Sci. Forum **196-201**, 167 (1995).
[5] P. Vanmeerbeek and P. Clauws, Phys. Rev. B **64**, 245201 (2001).
[6] V. P. Markevich, I. D. Hawkins, A. R. Peaker, V. V. Litvinov, L. I. Murin, L. Dobaczewski, and J. L. Lindström, Appl. Phys. Lett. **81**(10), 1821 (2002).
[7] J. Coutinho, R. Jones, P. R. Briddon, and S. Öberg, Phys. Rev. B **62**, 10 824 (2000).
[8] W. Kaiser, J. Phys. Chem. Solids **23**, 255 (1962).
[9] B. Pajot and P. Clauws, in *Proceedings of the 18th International Conference on the Physics of Semiconductors*, edited by O. Engström (World Scientific, Singapore, 1987), pp. 911–914.
[10] L. I. Khirunenko, V. I. Shakhovtsov, and V. K. Shinkarenko, Mater. Sci. Forum **83-87**, 425 (1992).
[11] A. J. Mayur, M. D. Sciacca, M. K. Udo, A. K. Ramdas, K. Itoh, J. Wolk, and E. E. Haller, Phys. Rev. B **49**, 16 293 (1994).
[12] B. Pajot, P. Clauws, J. L. Lindström, and E. Artacho, Phys. Rev. B **62**, 10 165 (2000).
[13] V. V. Litvinov, L. I. Murin, J. L. Lindström, V. P. Markevich, and A. N. Petukh, Semiconductors **36**, 621 (2002).
[14] P. Vanmeerbeek, P. Clauws, and W. Mondelaers, Physica B **308-310**, 517 (2001).
[15] G. Herzberg, *Molecular Spectra and Molecular Structure II. Infrared and Raman Spectra of Polyatomic Molecules* (Krieger, Malabar, 1991).
[16] V. V. Litvinov, V. I. Urenev, and V. A. Shershel', Sov. Phys. Semicond. **17** (9), 1033 (1983).
[17] V. V. Litvinov, V. I. Urenev, and V. A. Shershel', Sov. Phys. Semicond. **18** (6), 707 (1984).
[18] L. A. Goncharov, V. V. Emtsev, T. V. Mashovets, and S. M. Ryvkin, Sov. Phys. Semicond. **6** (2), 369 (1972).
[19] V. V. Litvinov, L. I. Murin, J. L. Lindström, V. P. Markevich, and A. A. Klechko, Solid State Phenom. **82-84**, 105 (2002).
[20] H. J. Stein, Appl. Phys. Lett. **48** (22), 1540 (1986).